Journal of Biomolecular NMR, **14:** 377–381, 1999.
KLUWER/ESCOM

2D and 3D TROSY-enhanced NOESY of ^{15}N labeled proteins

Guang Zhu*, Youlin Xia, Kong Hung Sze & Xiangzhong Yan
Department of Biochemistry, The Hong Kong University of Science and Technology, Clear Water Bay, Kowloon, Hong Kong

Received 10 May 1999; Accepted 7 July 1999

Key words: ^{15}N labeled proteins, NOESY, TROSY

Abstract

Recently, several TROSY-based experiments have been designed for backbone chemical shift assignment and measurement of the NOEs of ^{2}H, ^{13}C and ^{15}N labeled proteins. Here, we present TROSY-enhanced NOESY experiments, namely the 2D S3E-NOESY-S3E, 3D TROSY-NOESY-S3E and S3E-NOESY-TROSY experiments. These experiments use the spin-state selective excitation method (S3E), and have the TROSY effect in all the indirectly and directly detected dimensions, and so provide optimal resolution for amide protons. The first two experiments provide an additional useful feature in that the diagonal peaks of the amide proton region are cancelled or greatly reduced, allowing clear identification of NOE cross peaks that are close to diagonal peaks.

Recent developments in Transverse Relaxation Optimized Spectroscopy (TROSY) have made it possible to study large ^{15}N labeled biomolecules (>30 kDa) by exploiting the interference between chemical shift anisotropy and the dipole-dipole interaction between amide protons and their attached ^{15}N (Pervushin et al., 1997). Several TROSY-based experiments have already been designed for backbone chemical shift assignment of ^{2}H, ^{13}C and ^{15}N labeled proteins (Pervushin et al., 1998; Weigelt, 1998; Salzmann et al., 1998; Yang and Kay, 1998; Zhu et al., 1998). 3D NOESY-TROSY experiments have also been described (Brutscher et al., 1998; Zhu et al., 1999) to obtain structural information from ^{15}N labeled and partially deuterated proteins (Reisman et al., 1991; Nietlispach et al., 1996). Here, we present three enhanced NOESY-TROSY experiments, namely, the 2D S3E-NOESY-S3E, 3D TROSY-NOESY-S3E and S3E-NOESY-TROSY experiments with the use of the spin-state selective excitation method (S3E) (Meissner et al., 1997; Sørensen et al., 1997; Pervushin et al., 1998). These experiments have the TROSY effect in all the indirectly and directly detected dimensions, and so provide optimal resolution for amide protons. Furthermore, the first two experiments provide an additional useful feature in that the diagonal peaks of the amide proton region are cancelled or greatly reduced. This enables clear identification of NOESY cross peaks close to the diagonal.

The pulse sequences of 2D S3E-NOESY-S3E, 3D TROSY-NOESY-S3E and S3E-NOESY-TROSY experiments are depicted in Figures 1A to 1C, respectively. The section between points *a* and *b* in Figure 1A is a reversed INEPT (rev_INEPT) sequence designed so that ^{15}N steady state enhancement can be used in the 2D S3E-NOESY-S3E experiment. Sections between points *b* and *c*, and points *d* and *e* contain the S3E sequences which serve to select the component of the $^{1}H_N$ split peaks with the slower relaxation rate. The 2D S3E-NOESY-S3E experiment is a combination of the S3E method and the ordinary NOESY experiment. This experiment not only gives H_N-H_N and H_N-H_C NOE cross peaks with the characteristic narrow TROSY H_N linewidths and greatly reduced diagonal peaks, but also provides normal NOE cross peaks, although with reduced intensities. The evolution of the density operator from point *a* to *b* is as follows,

*To whom correspondence should be addressed. E-mail: gzhu@ust.hk

$$\begin{aligned}\sigma_a &= uI_z + vS_z \xrightarrow{\text{rev\_INEPT}} \sigma_b \\ &= -\left[(u+v)S_\alpha + (u-v)S_\beta\right] I_z\end{aligned}$$

where $S_\alpha = 0.5E + S_z$, $S_\beta = 0.5E - S_z$, u and v are the relative magnitudes of ^{1}H and ^{15}N steady state magnetizations, E is the identity matrix, and S_α and S_β correspond to the α and β states of the S nucleus, respectively. After the first S3E sequence (from point *b* to *c*), the density operator becomes

$$\begin{aligned}\sigma_c &= -\left[(u+v)S_\beta I_x + (u-v)S_\alpha I_y\right] \\ &\quad \text{when } \varphi_3 = \text{x}, \varphi_4 = \text{x}, \\ \sigma_c &= -\left[(u+v)S_\beta I_x - (u-v)S_\alpha I_y\right] \\ &\quad \text{when } \varphi_3 = \text{x}, \varphi_4 = -\text{x}\end{aligned}$$

The slowly relaxing component in the equations above can be obtained by adding two FIDs recorded with phases $\varphi_3 = (\text{x}, \text{x})$, $\varphi_4 = (\text{x}, -\text{x})$, with the rest of the phases being the same. The resulting σ_c is

$$\sigma_c = -(u+v)S_\beta I_x$$

Thus, we have not only selected the slowly relaxing component but also utilized the steady state magnetization of ^{15}N (Pervushin et al., 1998). The section between points *c* and *d* is the same as those in a normal 2D NOESY pulse sequence. The detected magnetization is filtered through the second S3E sequence to obtain TROSY ^1H_N components as expressed below with phases $\varphi_9 = (\text{x}, \text{x})$ and $\varphi_{10} = (\text{x}, -\text{x})$,

$$\sigma_e = -\eta(u+v)\sin\left[(\omega_I - \pi J)t_1\right] e^{i(\omega_{I'} - \pi J)t_2} S_\alpha S'_\beta I'_-$$

where η is the NOE transfer factor, ω_I is the chemical shift of spin I, J is the one-bond coupling constant between ^{1}H and ^{15}N, spin I' with chemical shift $\omega_{I'}$ is connected to spin I through an NOE contact, and spin S' is connected to spin I' through J coupling. Another quadrature component is obtained by increasing the phases of φ_1 to φ_4 by 90°. For diagonal peaks,

$$\sigma_e = -(u+v)\sin\left[(\omega_I - \pi J)t_1\right] e^{i(\omega_I - \pi J)t_2} S_\alpha S_\beta I_-$$

The intensities of the diagonal peaks are zero since $S_\alpha S_\beta = 0$. In practice, some residual diagonal peaks

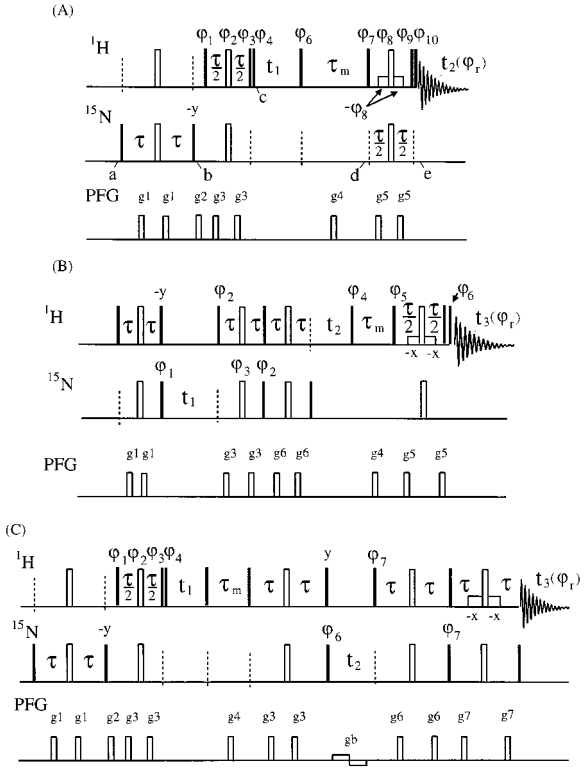

Figure 1. 2D and 3D TROSY-enhanced NOESY pulse sequences. Filled bars and open bars represent 90° and 180° pulses, respectively. Default phases are in the x direction. The experimental recovery delay is 1 s, $\tau = 1/(4^1J_{NH}) \approx 2.7$ ms, $\tau_m = 80$ ms. (A) S3E-NOESY-S3E pulse sequence: $\varphi_1 = (\text{x},-\text{x},-\text{x},\text{x},\text{y},-\text{y},-\text{y},\text{y}) + 45°$; $\varphi_2 = 4(\text{y}),4(-\text{x})$; $\varphi_3 = 4(\text{x}),4(\text{y})$; $\varphi_4 = (\text{x},-\text{x},\text{x},-\text{x},\text{y},-\text{y},\text{y},-\text{y})$; $\varphi_6 = 4(\text{x}), 4(\text{y})$; $\varphi_7 = [16(\text{x}),16(\text{y}), 16(-\text{x}),16(-\text{y})] + 45°$; $\varphi_8 = 16(\text{y}),16(-\text{x})$; $\varphi_9 = 16(\text{x}),16(\text{y})$; $\varphi_{10} = 8(\text{x}), 8(-\text{x}), 8(\text{y}), 8(-\text{y})$; $\varphi_r = 4(\text{x},-\text{x},-\text{x},\text{x}), 4(\text{y},-\text{y},-\text{y},\text{y}), 4(-\text{x},\text{x},\text{x},-\text{x}), 4(-\text{y},\text{y},\text{y},-\text{y})$. The quadrature component in the t_1 dimension is acquired by altering the phases φ_1 to φ_4 in the States-TPPI manner. (B) TROSY-NOESY-S3E pulse sequence: $\varphi_1 = (\text{x},\text{y},-\text{x},-\text{y})$; $\varphi_2 = (\text{y})$; $\varphi_3 = (\text{x})$; $\varphi_4 = (\text{x},\text{y})$; $\varphi_5 = [4(\text{x}),4(-\text{x})] + 45°$; $\varphi_6 = 8(\text{x}), 8(-\text{x})$; $\varphi_{10} = (-\text{x},\text{x})$; $\varphi_r = (\text{x},\text{x},-\text{x},-\text{x},-\text{x},\text{x},\text{x})$. Four transients, $S_{\text{phase1,phase2}}$, are acquired through altering φ_2 and φ_4 (if phase1 = 2, $\varphi_2 = \varphi_2 + 180°$ and $\varphi_4 = \varphi_4 + \varphi_{10}$, else φ_2 and φ_4 are unchanged; if phase2 = 2, $\varphi_4 = \varphi_4 - 90°$, else φ_4 is unchanged) for every pair of t_1 and t_2 values. Axial peaks are removed by setting phases ($\varphi_1 + 180°$, $\varphi_r + 180°$) and ($\varphi_3 + 90°$, $\varphi_r + 180°$) for every second t_1 and t_2 increment, respectively. The transmitter offset for proton before the NOE mixing period is set at 8.5 ppm. (C) S3E-NOESY-TROSY pulse sequence: $\varphi_1 = (\text{x},-\text{x},-\text{x},\text{x}) + 45°$; $\varphi_2 = (\text{y})$; $\varphi_3 = (\text{x})$; $\varphi_4 = (\text{x},-\text{x})$; $\varphi_6 = 4(\text{y}), 4(\text{x}), 4(-\text{y}),4(-\text{x})$; $\varphi_7 = (\text{y})$; $\varphi_{10} = 4(\text{x}), 4(-\text{x}), 4(\text{x}), 4(-\text{x})$; $\varphi_r = (\text{x},-\text{x},-\text{x},\text{x},-\text{y},\text{y},\text{y},-\text{y},-\text{x},\text{x}, \text{x},-\text{x},\text{y},-\text{y},-\text{y},\text{y})$. Four transients, $S_{\text{phase1,phase2}}$, are recorded through altering the phases φ_1 to φ_4, φ_r and φ_7 (if phase1 = 2, φ_1 to φ_4 plus 90°, else φ_1 to φ_4 unchanged; if phase2 = 2, $\varphi_r = \varphi_r + \varphi_{10}$, $\varphi_7 = \varphi_7 + 180°$, else φ_r and φ_7 unchanged) for every pair of t_1 and t_2 values. Axial peaks are removed by setting ($\varphi_6 + 180°$, $\varphi_r + 180°$) for every second t_2 increment. The final absorption mode spectra of pulse sequences (B) and (C) are obtained with the use of the methods stated in the text. The durations and strengths of the gradients are g1 = (0.4 ms, 5 G/cm); g2 = (0.4 ms, 15 G/cm); g3 = g1; g4 = (4 ms, 25 G/cm); g5 = (0.4 ms, 25 G/cm); g6 = g1; g7 = (0.4 ms, 8 G/cm), gb is a small bipolar gradient.

may still be present in the spectra. The residual diagonal peaks come from the relaxation of S_z magnetization during the NOE mixing time τ_m. The intensities of residual diagonal peaks are proportional to $1 - \exp(-\tau_m/T_{1S})$, where T_{1S} is the longitudinal relaxation time of the S spin. If $\tau_m = 0.05$ s and $T_{1S} = 0.5$ s, these intensities are about 10% of that of the corresponding diagonal peaks in a normal 2D NOESY spectrum. By taking into account the $^1J_{HN}$ splittings of the diagonal peaks originating from imperfections in the settings of S3E, the magnetization at point *c* can be expressed as

$$\sigma_c = -(u + v)\left[S_\beta I_x + \delta S_\alpha I_x\right],$$

where $\pi J\tau = 45^\circ + \delta$, and δ is a small quantity. A rapidly relaxing component, $\delta S_\alpha I_x$, with its intensity being proportional to δ, will be present. Due to variation in $^1J_{HN}$, there will always be some rapidly relaxing components, $\delta S_\alpha I_x$ with their intensities being comparable to that of the NOE cross peaks. In order not to obscure the NOE peaks, we can set $\pi J\tau$ to be less than 45° ($\delta < 0$) so that the artifacts given by this term will be negative when compared with the NOE peaks. It should be noted that non-amide protons can also go through S3E, and so provide NOE cross peaks and structural information.

Figure 1B describes a 3D TROSY-NOESY-S3E experiment. The selection of the slowly relaxing components of ^{1}H and ^{15}N magnetization before the NOE mixing time is realized by the use of the ^{15}N-^{1}H TROSY scheme, and the selection of the TROSY ^{1}H component before detection is accomplished by the use of the S3E sequence. Thus the characteristic TROSY spectral linewidths are obtained in all three dimensions of the 3D spectrum. As in the 2D S3E-NOESY-S3E experiment, the diagonal peaks in the H_N-H_N region will be cancelled or greatly reduced. It is expected that this experiment and the 2D S3E-NOESY-S3E will be extremely useful for large biomolecules labeled with ^{15}N and partially labeled with ^{2}H when normal NOESY experiments become impractical. In the 3D TROSY-NOESY-S3E experiment some H_N-H_α NOE cross peaks may be obscured due to insufficient water suppression by the S3E used here. One alternative is to use the S3E-NOESY-TROSY experiment as depicted in Figure 1C. The main features of this experiment are that the diagonal peaks are of TROSY linewidth (but are not cancelled or reduced as in the TROSY-NOESY-S3E experiment), and the H_N-H_α NOESY cross peaks are easily identified due to the better water suppression afforded by TROSY (Zhu et al., 1999). If only the H_N-H_N NOESY cross peaks are of interest, the TROSY-NOESY-S3E experiment is the better choice due to the cancellation or strong reduction of the diagonal peaks. Otherwise, the S3E-NOESY-TROSY experiment may be preferred.

Note that for the proposed 3D experiments, the minimum number of phase cycling steps that could be used is 4. Two steps are required for the selection of the slowly relaxing components in the TROSY section, and two steps are needed for the S3E segment. However, the sensitivity of the 4-step phase cycle is only 50% of that of the 16-step cycle. If the sample concentration is high, the 4-step phase cycle scheme can be used so that sufficient increments in t_1 and t_2 can be collected in a reasonable amount of time to increase the digital resolution.

When the coherence of H_N or H_C goes through one S3E sequence, the intensities of H_N signals will decrease by 50% because, like TROSY, S3E only selects one component of the magnetization, and the coherence of H_C signals will decrease by 28% because the phases of φ_1 or φ_7 are 45°. Therefore, the sensitivities of these experiments are reduced by 75% for H_N-H_N cross peaks, by 64% for H_N-H_C cross peaks and by 50% for H_C-H_C cross peaks when compared with the corresponding normal 2D NOESY and 3D sensitivity enhanced NOESY-HSQC experiments.

For the 3D TROSY-NOESY-S3E experiment, a different phase cycling scheme from that of the original 2D TROSY experiment has to be employed because the NOESY section cannot transfer two orthogonal components simultaneously. The four recorded transients used to construct an absorption mode spectrum are:

$$S_{11} = \sin\left[(\omega_S + \pi J)t_1 + (\omega_I - \pi J)t_2\right] e^{i(\omega_{I'} - \pi J)t_3}$$
$$S_{12} = \cos\left[(\omega_S + \pi J)t_1 + (\omega_I - \pi J)t_2\right] e^{i(\omega_{I'} - \pi J)t_3}$$
$$S_{21} = \sin\left[-(\omega_S + \pi J)t_1 + (\omega_I - \pi J)t_2\right] e^{i(\omega_{I'} - \pi J)t_3}$$
$$S_{22} = \cos\left[-(\omega_S + \pi J)t_1 + (\omega_I - \pi J)t_2\right] e^{i(\omega_{I'} - \pi J)t_3}$$

The real and imaginary parts, S'_{ij}, of the FID can be obtained as follows:

$$S'_{11} = S_{22} + S_{12}$$
$$S'_{12} = S_{11} + S_{21}$$
$$S'_{21} = S_{11} - S_{21}$$
$$S'_{22} = S_{22} - S_{12}$$

The spectrum can then be obtained by using a normal Fourier transformation scheme. In the case of the 3D S3E-NOESY-TROSY experiment, the four recorded transients can be expressed as:

$$
\begin{aligned}
S_{11} &= \sin[(\omega_I - \pi J)t_1]\, e^{i[(\omega_{S'}+\pi J)t_2+(\omega_{I'}-\pi J)t_3]} \\
S_{12} &= \sin[(\omega_I - \pi J)t_1]\, e^{i[-(\omega_{S'}+\pi J)t_2+(\omega_{I'}-\pi J)t_3]} \\
S_{21} &= \cos[(\omega_I - \pi J)t_1]\, e^{i[(\omega_{S'}+\pi J)t_2+(\omega_{I'}-\pi J)t_3]} \\
S_{22} &= \cos[(\omega_I - \pi J)t_1]\, e^{i[-(\omega_{S'}+\pi J)t_2+(\omega_{I'}-\pi J)t_3]}
\end{aligned}
$$

and the FID components, S'_{ij}, before Fourier transformation can be expressed as follows:

$$
\begin{aligned}
S'_{11} &= S_{21} + S_{22} \\
S'_{12} &= S_{21} - S_{22} \text{ (with a 90° phase shift)} \\
S'_{21} &= S_{11} + S_{12} \\
S'_{22} &= S_{11} - S_{12} \text{ (with a 90° phase shift).}
\end{aligned}
$$

To demonstrate the effectiveness of these experiments, we applied the 2D and 3D TROSY-enhanced NOESY experiments to a ^{15}N labeled *Xenopus laevis* Calmodulin sample (16.7 kDa, 1.5 mM at pH 6.3 and 25 °C, 6.1 mM $CaCl_2$ and 0.1 M KCl) on a Varian Inova 750 MHz NMR spectrometer. Figures 2A and 2B show the amide proton regions of a conventional 2D NOESY spectrum and the 2D S3E-NOESY-S3E spectrum, respectively. It is clear that the diagonal peaks from Figure 2B are cancelled or greatly reduced in the H_N region of the spectrum, revealing more cross peaks with enhanced resolution when compared with the normal NOESY spectrum (Figure 2A). The linewidths in Figure 2B are about 4 Hz narrower on average than those in Figure 2A. The open contours near the diagonal peaks in Figure 2B are the negative $^1J_{HN}$ splittings of the diagonal peaks, which are generated as discussed previously.

Figure 2C displays the 2D NOESY spectrum obtained by projecting 2D ^{1}H-^{1}H cross sections of the 3D TROSY-NOESY-S3E spectrum along the ^{15}N dimension. Figure 2D depicts the first 2D ^{1}H-^{1}H plane from the 3D S3E-NOESY-TROSY experiment with the setting $t_2 = 0$ to show the water suppression capability of this experiment. As seen in Figure 2C, the 3D TROSY-NOESY-S3E experiment can produce a spectrum with cancelled or greatly reduced diagonal peaks in the H_N region, but with some loss of cross peaks in the H_N-H_α region due to the water suppression scheme used in the S3E. The cross peaks in the H_N-H_α region

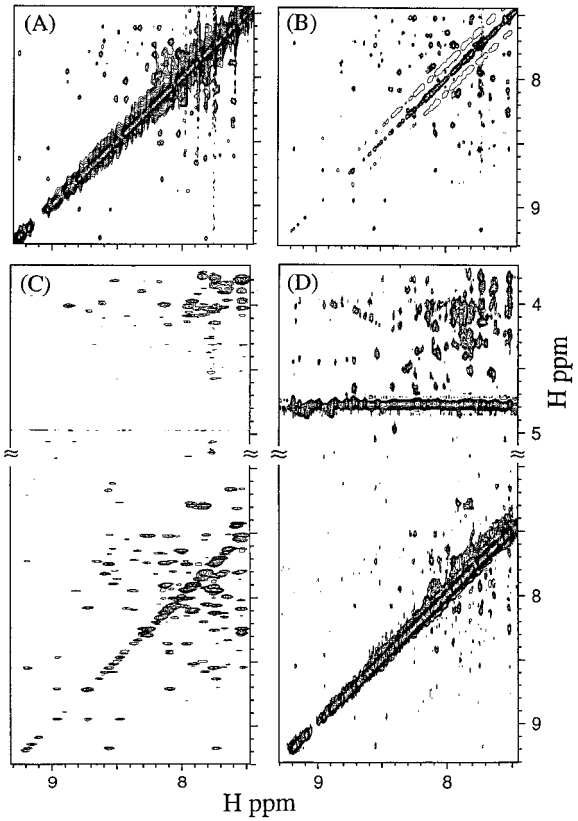

Figure 2. 2D and 3D TROSY-enhanced NOESY spectra. (A) and (B): Amide proton regions of a normal 2D NOESY spectrum and the S3E-NOESY-S3E 2D spectrum, respectively. Spectral widths in both dimensions are 10500 Hz. 600 FIDs were acquired, each with 64 transients. The NOESY peaks in (B) are 45 Hz offset when compared with those of (A) due to the TROSY selection. (C) The 2D spectrum obtained by the projection of 2D ^{1}H-^{1}H cross-sections of the 3D TROSY-NOESY-S3E spectrum along the ^{15}N dimension. For the 3D spectrum, 64(^{15}N)×128(^{1}H) FIDs were recorded, each with 16 scans. Spectral widths in three dimensions are 3000 Hz (^{15}N), 4500 Hz (^{1}H) and 10500 Hz (^{1}H). Note that the transmitter offset of proton is shifted to 8.5 ppm in the F1 dimension. (D) The first 2D ^{1}H-^{1}H plane obtained from the 3D S3E-NOESY-TROSY experiment using 600 FIDs, each with 64 scans and $t_2 = 0$. Spectral widths in the three dimensions are 10500 Hz (^{1}H), 3000 Hz (^{15}N) and 10500 Hz (^{1}H).

can be obtained with the use of a 3D S3E-NOESY-TROSY experiment (Figure 2D). The experimental data matrices used for obtaining the above spectra were $300^* \times 2048^*$ and $32^* \times 64^* \times 256^*$, where '*' denotes complex number. The spectra were processed by using only regular cosine-bell window functions and Fourier transformation (States et al., 1982; Delaglio et al., 1995; Zhu et al., 1998).

In summary, we have presented 2D S3E-NOESY-S3E, 3D TROSY-NOESY-S3E and S3E-NOESY-

TROSY experiments which have been applied to ^{15}N labeled calmodulin. These experiments offer optimal resolution in all the indirectly and directly detected dimensions, with an additional feature that the diagonal peaks of the first two experiments are greatly suppressed in the amide proton region. If the $^{1}H_N$-$^{1}H_\alpha$ NOESY peaks need to be identified, 3D S3E-NOESY-TROSY can be applied for its superior ability to reveal NOE cross peaks close to the water resonance. Further improvements in water suppression in the TROSY-NOESY-S3E may be possible by adding a WATERGATE sequence after the S3E, but this could result in a decrease in sensitivity. The drawback of these experiments is that they are less sensitive than the corresponding normal 2D NOESY and 3D NOESY-HSQC experiments. However, this sensitivity loss is compensated for by the narrower spectral linewidths afforded by TROSY for large proteins (Pervushin et al., 1997). Partial deuteration of proteins can largely reduce the contributions of ^{1}H-^{1}H and ^{1}H-^{15}N dipolar interactions to the relaxation of the amide proton and nitrogen, so that the TROSY effect is enhanced (Ishima et al., 1998; Salzmann et al., 1998). We expect that the experiments demonstrated here will have application when conventional NOESY experiments become impractical as the molecular weights of the proteins or nucleic acids being studied increase.

Acknowledgements

This work is supported by grants from the Research Grant Council of Hong Kong (HKUST6197/97M and HKUST6038/98M). We also thank Dr. Mingjie Zhang for providing the ^{15}N labeled calmodulin, and Dr. D.K. Smith for critical discussions. The Hong Kong Biotechnology Research Institute is acknowledged for the purchase of the 750 MHz NMR spectrometer.

References

Brutscher, B., Boisbouvier, J., Pardi, A., Marion, D. and Simorre, J.P. (1998) *J. Am. Chem. Soc.*, **120**, 11845–11851.

Delaglio, F., Grzesiek, S., Vuister, G.W., Zhu, G., Pfeifer, J. and Bax, A. (1995) *J. Biomol. NMR*, **6**, 277–293.

Ishima, R., Wingfield, P.T., Stahl, S.J., Kaufman, J.D. and Torchia, D.A. (1998) *J. Am. Chem. Soc*., **120**, 10534–10542.

Meissner, A., Duus, J.Ø. and Sørensen, O.W. (1997) *J. Biomol. NMR*, **10**, 89–94.

Nietlispach, D., Clowes, R.T., Broadhurst, R.W., Ito, Y., Keeler, J., Kelly, M., Ashurst, J., Oschkinat, H., Domaille, P.J. and Laue, E.D. (1996) *J. Am. Chem. Soc*., **118**, 407–415.

Pervushin, K., Riek, R., Wider, G. and Wüthrich, K. (1997) *Proc. Natl. Acad. Sci. USA*, **94**, 12366–12371.

Pervushin, K., Riek, R., Wider, G. and Wüthrich, K. (1998) *J. Am. Chem. Soc.*, **120**, 6394–6400.

Reisman, J., Jariel-Encontre, I., Hsu, V.L., Parello, J., Geiduschek, E.P. and Kearns, D.R. (1991) *J. Am. Chem. Soc.*, **113**, 2787–2789.

Salzmann, M., Pervushin, K., Wider, G., Senn, H. and Wüthrich, K. (1998) *Proc. Natl. Acad. Sci. USA*, **95**, 13585–13590.

Sørensen, M.D., Meissner, A. and Sørensen, O.W. (1997) *J. Biomol. NMR*, **10**, 181–186.

States, D.I., Haberkorn, R.A. and Ruben, D.J. (1982) *J. Magn. Reson.*, **93**, 151.

Weigelt, J. (1998) *J. Am. Chem. Soc*., **120**, 10778–10779.

Yang, D. and Kay, L.E. (1999) *J. Biomol. NMR*, **13**, 3–10.

Zhu, G., Kong, X.M., Yan, X.Z. and Sze, K.H. (1998) *Angew. Chem. Int. Ed. Engl.*, **37**, 2859–2861.

Zhu, G., Kong, X.M. and Sze, K.H. (1999) *J. Biomol. NMR*, **13**, 77–81.